

Distribution-Free Bayesian multivariate predictive inference

Daniel Yekutieli

October 15, 2021

Abstract

We introduce a comprehensive Bayesian multivariate predictive inference framework. The basis for our framework is a hierarchical Bayesian model, that is a mixture of finite Polya trees corresponding to multiple dyadic partitions of the unit cube. Given a sample of observations from an unknown multivariate distribution, the posterior predictive distribution is used to model and generate future observations from the unknown distribution. We illustrate the implementation of our methodology and study its performance on simulated examples. We introduce an algorithm for constructing conformal prediction sets, that provide finite sample probability assurances for future observations, with our Bayesian model.

1 Introduction

The predictive distribution is an important feature of Bayesian analyses that is typically used as a diagnostic tool for assessing model fit. In this work we apply a hierarchical Bayesian model, that is a mixture of finite Polya trees corresponding to multiple dyadic partitions of $[0, 1]^P$, to a sample of iid observations from an unknown distribution $\tilde{\pi}$. The resulting posterior predictive distribution is used to approximate the distribution of future observations from $\tilde{\pi}$.

The use of finite Polya trees to define random distributions on dyadic partitions of the unit interval was introduced in Ferguson (1974). The theoretical properties of Polya tree models for density estimation has been widely studied. Use of Polya trees, corresponding to multiple dyadic partitions, for distribution-free estimation of multivariate densities was suggested in Wong and Ma (2010) and Ma (2017). The novel features of this work is the introduction of a hierarchical Bayesian model that assigns distributions to sets of dyadic partitions of $[0, 1]^P$; the introduction and implementation of a comprehensive Bayesian predictive inference framework; the adaptation of the Vovk (2005) method for constructing Conformal prediction sets to Bayesian analyses.

In Section 2 we present our inferential framework. In Sections 3, 4, 5, we illustrate the use of our methodology and study its performance on simulated examples. In Section 3 we study how well our model approximates and estimates one-dimensional and two-dimensional densities. In Section 4 we apply our method for quantile regression for a two-dimensional density, and introduce and implement an algorithm for constructing Conformal prediction sets with our Bayesian model. In Section 5 we attempt to scale up our methodology to provide predictive inference for a sample of 8 continuous variables and one categorical variable. In Section 6 we discuss our work and outline changes needed to make it applicable in high dimensional problems.

2 Hierarchical Bayesian modelling for predictive inference

2.1 Dyadic segmentations of the P -dimensional unit cube

L level dyadic segmentations are constructed by partitioning the unit cube, $\mathcal{I}_0 = [0, 1]^P$, L times in half according to its P dimensions. Each segmentation, $\vec{\mathcal{I}} = \{\mathcal{I}_{l,j}\}_{l=1 \dots L}^{j=1 \dots 2^{l-1}}$, consists of $2 \cdot (2^L - 1)$ subintervals specified by a segmentation ordering vector, $\vec{d} = \{d_{l,j}\}_{l=1 \dots L}^{j=1 \dots 2^{l-1}}$ with $d_{l,j} \in \{1, \dots, P\}$. The segmentation begins by partitioning \mathcal{I}_0 according to Dimension $d_{1,1}$ into two halves, $\mathcal{I}_{1,1}(\vec{d})$ that consists of the small values of coordinate $d_{1,1}$ and $\mathcal{I}_{1,2}(\vec{d})$ that consists of the large values of coordinate $d_{1,1}$. And then, for $l = 2 \dots L$ and $j = 1 \dots 2^{l-1}$, $\mathcal{I}_{l-1,j}(\vec{d})$ is partitioned in half according to coordinate $d_{l,j}$ into $\mathcal{I}_{l,2 \cdot j-1}(\vec{d})$ consisting of small values of coordinate $d_{l,j}$ and into $\mathcal{I}_{l,2 \cdot j}(\vec{d})$ consisting of large values of coordinate $d_{l,j}$.

In the segmentations we consider in the examples in this report, all the subintervals at the same level are partitioned according to the same dimension (i.e. $d_{l,j}$ is the same $\forall j$). In which case, \vec{d} is given by $(d_1 \dots d_L)$.

In Figure 1 we display four $L = 4$ level dyadic segmentations of $[0, 1]^2$ into $16 = 2^4$ subintervals. Setting the X axis to be Dimension 1 and the Y axis to be Dimension 2, the segmentation with all $d_{l,j} = 1$ is denoted by (X, X, X, X) ; the segmentation with all $d_{l,j} = 2$ is denoted by (Y, Y, Y, Y) ; while the segmentation with $d_{1,j} = 1$, $d_{2,j} = 1$, $d_{3,j} = 2$ and $d_{4,j} = 2$ is denoted (X, X, Y, Y) . The numbers in each subinterval mark the positions of the level $L = 4$ subintervals, $\mathcal{I}_{4,1}(\vec{d}) \dots \mathcal{I}_{4,16}(\vec{d})$, for each segmentation.

2.2 The hierarchical Beta model

The L level hierarchical Beta (hBeta) model is a finite Polya tree model that generates random densities that are step functions on $\{\mathcal{I}_{L,1}, \dots, \mathcal{I}_{L,2^L}\}$ for a given L level segmentation \vec{d} . The parameters of the hBeta model are Beta distribution hyper-parameters, $\alpha_{l,j}$ and $\beta_{l,j}$ for $l = 1 \dots L$ and $j = 1 \dots 2^{l-1}$. The hBeta model generates the following components.

a. Independent Beta random variables. $\phi_{l,j} \sim \text{Beta}(\alpha_{l,j}, \beta_{l,j})$, for $l = 1 \dots L$ and $j = 1 \dots 2^{l-1}$. The Beta random variables specify the conditional subinterval probabilities. $\Pr(\mathcal{I}_{1,1}|\mathcal{I}_0) = \phi_{1,1}$ and $\Pr(\mathcal{I}_{1,2}|\mathcal{I}_0) = 1 - \phi_{1,1}$. For $l = 2 \dots L$ and $j = 1 \dots 2^{l-1}$, $\Pr(\mathcal{I}_{l,2 \cdot j-1}|\mathcal{I}_{l-1,j}) = \phi_{l,j}$ and $\Pr(\mathcal{I}_{l,2 \cdot j}|\mathcal{I}_{l-1,j}) = 1 - \phi_{l,j}$.

b. Subinterval probabilities. The subinterval probabilities, $\Pr(\mathcal{I}_{l,j}) = \pi_{l,j}$, are products of the conditional subinterval probabilities. $\pi_{1,1} = \phi_{1,1}$ and $\pi_{1,2} = 1 - \phi_{1,1}$. For $l = 2 \dots L$ and $j = 1 \dots 2^{l-1}$, $\pi_{l,2 \cdot j-1} = \phi_{l,j} \cdot \pi_{l-1,j}$ and $\pi_{l,2 \cdot j} = (1 - \phi_{l,j}) \cdot \pi_{l-1,j}$.

c. Step function PDF. The components of $\vec{\pi}_L = (\pi_{L,1} \dots \pi_{L,2^L})$ specify the step function PDF,

$$f(u|\vec{d}, \vec{\pi}_L) = \pi_{L,1} \cdot \frac{I_{L,1}(u; \vec{d})}{(1/2)^L} + \dots + \pi_{L,2^L} \cdot \frac{I_{L,2^L}(u; \vec{d})}{(1/2)^L}, \quad (1)$$

for $u \in [0, 1]^P$ and with $I_{l,j}(u; \vec{d})$ denoting the indicator function corresponding to subinterval $\mathcal{I}_{l,j}(\vec{d})$.

In Figure 2 we provide a schematic for the hierarchical Beta model with $L = 3$ levels.

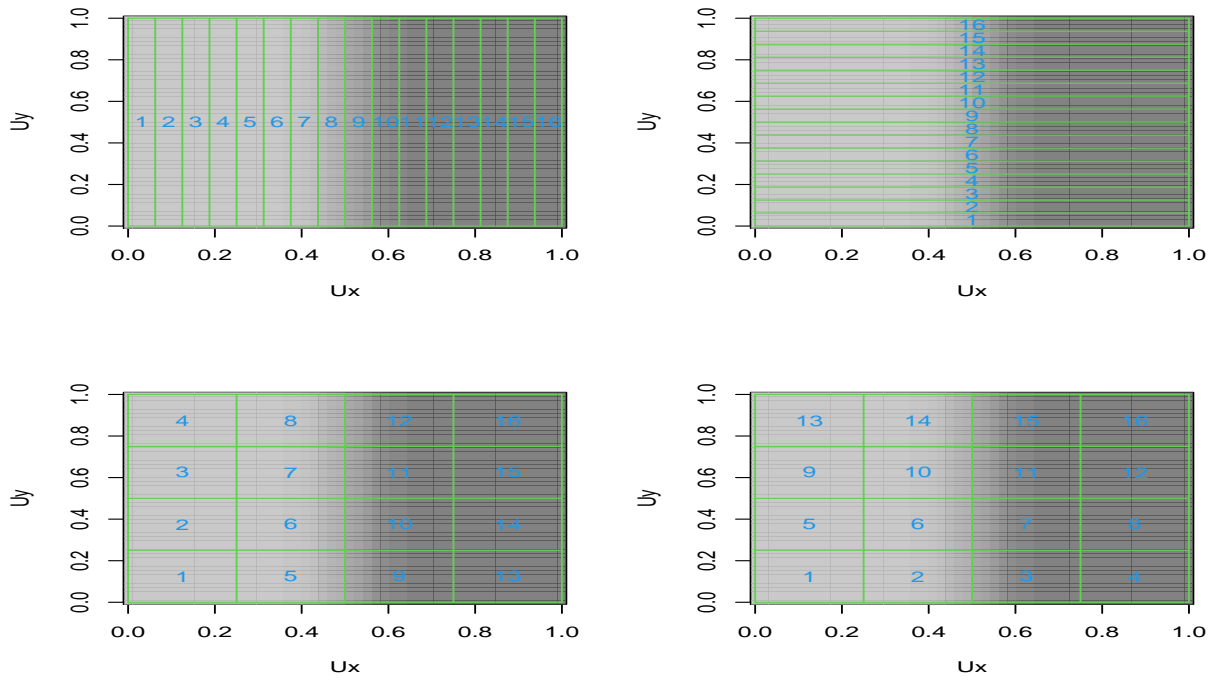


Figure 1: 4 level dyadic segmentations of $[0, 1]^2$. The top left plot displays segmentation (X, X, X, X) ; the top right plot displays segmentation (Y, Y, Y, Y) ; the bottom left plot displays segmentation (X, X, Y, Y) ; the bottom right plot displays segmentation (Y, Y, X, X) . The blue numbers in each plot mark the positions of the level 4 subintervals, $\mathcal{I}_{4,1} \cdots \mathcal{I}_{4,16}$, for each segmentation. The gray shading in all the plots displays density $\tilde{\pi}(u_x, u_y) = 2 \cdot \text{logit}^{-1}(20 \cdot (u_x - 0.5))$.

2.3 The hierarchical Bayesian framework

Let $u_1 \cdots u_m$ denote the sample of iid observations from $\tilde{\pi}$. On observing data points $u_1 \cdots u_m$, our goal is to provide inference regarding an unobserved data point u_{m+1} , that is assumed to be also independently sampled from $\tilde{\pi}$. To drive our inferential framework, we elicit the following generative model for $u_1 \cdots u_{m+1}$.

Definition 2.1 Generative model for data

1. Sample \vec{d} with probability $1/|\mathcal{D}|$ from a given set of level L segmentations \mathcal{D} .
2. Generate $f(u|\vec{d}, \vec{\pi}_L)$ from the hBeta model with $\phi_{l,j} \sim \text{Beta}(1, 1)$, for $l = 1 \cdots L$ and $j = 1 \cdots 2^{l-1}$.
3. For $k = 1 \cdots m + 1$, generate $u_k \sim f(u|\vec{d}, \vec{\pi}_L)$.

Example 2.2 In Figure 3 we display the distribution of the CDF of $f(u|\vec{d}, \vec{\pi}_L)$ in Model 2.1, for the 10 level segmentation of $[0, 1]$, with subintervals $\mathcal{I}_{10,j} = [\frac{j-1}{1024}, \frac{j}{1024}]$ for $j = 1 \cdots 1024$, for $a_0 = 0.1, 1, 10$. In Model 2.1, $\phi_{l,j}$ are iid with $E\phi_{l,j} = a_0/(a_0 + a_0) = 1/2$, therefore $E\pi_{L,j} = (1/2)^L$, and thus the expectation of $f(u|\vec{d}, \vec{\pi}_L)$ is the $U[0, 1]$ density.

The plots reveal that increasing a_0 decreases the dispersion of $f(u|\vec{d}, \vec{\pi}_L)$. For $a_0 = 0.1$, the probabilities in $\vec{\pi}_{10}$ are concentrated – very unevenly – in a few very small clusters of contiguous subintervals. For $a_0 = 10$, the distribution of $\vec{\pi}_{10}$ is spread out in large clusters of similarly probable contiguous subintervals. While for $a_0 = 1$, the distribution of $\vec{\pi}_{10}$ consists of large clusters of low probability contiguous subintervals and a few small clusters of contiguous high probability subintervals.

2.3.1 The posterior data model

In this subsection we derive the conditional distribution given $\vec{u} = (u_1 \cdots u_m)$, of \vec{d} and the vector of Beta parameters, $\vec{\phi} = \{\phi_{l,j}\}_{l=1 \cdots L}^{j=1 \cdots 2^{l-1}}$, for Model 2.1.

For $\vec{d} \in \mathcal{D}$, $k = 1 \cdots m$, $l = 1 \cdots L$, $j = 1 \cdots 2^l$, let $N_{l,j}^k = I_{l,j}(u_k; \vec{d})$ denote the indicator variable for the event $u_k \in \mathcal{I}_{l,j}(\vec{d})$. The number of observations in subinterval $\mathcal{I}_{l,j}(\vec{d})$ is $N_{l,j}(\vec{u}; \vec{d}) = \sum_{k=1}^m N_{l,j}^k$. Conditional on $\vec{\phi}$, $N_{1,1} \sim \text{Binomial}(m, \phi_{1,1})$ and $N_{1,2} = m - N_{1,1}$. For $l = 2 \cdots L$ and $j = 1 \cdots 2^{l-1}$, conditioning on $\vec{\phi}$ and on $N_{l-1,j}$, $N_{l,2 \cdot j-1} \sim \text{Binomial}(N_{l-1,j}, \phi_{l,j})$ and $N_{l,2 \cdot j} = N_{l-1,j} - N_{l,2 \cdot j-1}$. Recalling that $\phi_{l,j} \sim \text{Beta}(a_0, a_0)$ and denoting $\vec{N}_{*,*} = \{N_{l,j}\}_{l=1 \cdots L}^{j=1 \cdots 2^l}$, this implies that $\phi_{l,j} | \vec{N}_{*,*}, \vec{d} \sim \text{Beta}(a_0 + N_{l,2 \cdot j-1}, a_0 + N_{l,2 \cdot j})$.

Ferguson (1974) has already noted the conjugacy of the conditional distribution of $\vec{\phi}$ given \vec{d} and \vec{u} for the hBeta model. In our inferential framework, the segmentation is random and we consider the conditional distribution of $\vec{\phi}$ and \vec{d} given \vec{u} . Denoting $\vec{N}_{L,*} = \{N_{L,j}\}_{j=1 \cdots 2^L}$ and $\vec{N}_{L,*}^k = \{N_{L,j}^k\}_{k=1 \cdots m}^{j=1 \cdots 2^L}$,

we begin by deriving the conditional distribution of \vec{d} .

$$\begin{aligned}
\Pr(\vec{d}|\vec{u}) &= \frac{f(\vec{d}, \vec{u})}{f(\vec{u})} = \frac{f(\vec{d}, \vec{u})}{\sum_{\vec{d}' \in \mathcal{D}} f(\vec{d}', \vec{u})} \\
&= \frac{f(\vec{N}_{L,*}^*, \vec{N}_{L,*}, \vec{d}, \vec{u})}{\sum_{\vec{d}' \in \mathcal{D}} f(\vec{N}_{L,*}^*, \vec{N}_{L,*}, \vec{d}', \vec{u})} \\
&= \frac{f(\vec{u}|\vec{N}_{L,*}^*, \vec{N}_{L,*}, \vec{d}) \cdot \Pr(\vec{N}_{L,*}^*|\vec{N}_{L,*}, \vec{d}) \cdot \Pr(\vec{N}_{L,*}|\vec{d}) \cdot \Pr(\vec{d})}{\sum_{\vec{d}' \in \mathcal{D}} f(\vec{u}|\vec{N}_{L,*}^*, \vec{N}_{L,*}, \vec{d}') \cdot \Pr(\vec{N}_{L,*}^*|\vec{N}_{L,*}, \vec{d}') \cdot \Pr(\vec{N}_{L,*}|\vec{d}') \cdot \Pr(\vec{d}')} \\
&= \frac{\Pr(\vec{N}_{L,*}^*|\vec{N}_{L,*}, \vec{d}) \cdot \Pr(\vec{N}_{L,*}|\vec{d})}{\sum_{\vec{d}' \in \mathcal{D}} \Pr(\vec{N}_{L,*}^*|\vec{N}_{L,*}, \vec{d}') \cdot \Pr(\vec{N}_{L,*}|\vec{d}')} \tag{2}
\end{aligned}$$

where the equality in (2) is because $\Pr(\vec{d}') \equiv 1/|\mathcal{D}|$ and $f(\vec{u}|\vec{N}_{L,*}^*, \vec{N}_{L,*}, \vec{d}') = (2^L)^m$. The latter holds because given \vec{d}' and $\vec{N}_{L,*}^*$, the components of \vec{u} are independently and Uniformly distributed within their respective level L subintervals, and each level L subintervals for each \vec{d}' has volume $(1/2)^L$. There are $\binom{m}{N_{L,1}, \dots, N_{L,2^L}} = m! / (\prod_{j=1}^{2^L} N_{L,j}!)$ different indicator vector instances $\vec{N}_{L,*}^*$ that yield the same counts vector $\vec{N}_{L,*}$. As the components of \vec{u} are exchangeable in Model 2.1 then each instance of $\vec{N}_{L,*}^*$ is equally probable, thfore

$$\Pr(\vec{N}_{L,*}^*|\vec{N}_{L,*}, \vec{d}') = \frac{\prod_{j=1}^{2^L} N_{L,j}!}{m!}. \tag{3}$$

Note that for each segmentation \vec{d} , $N_{1,1} \sim \text{Beta-Binomial}(m, a_0, a_0)$, $N_{1,2} = m - N_{1,1}$, and for $l = 2 \cdots L$ and $j = 1 \cdots 2^{l-1}$, $N_{l,2^j-1}|N_{l-1,j} \sim \text{Beta-Binomial}(N_{l-1,j}, a_0, a_0)$ and $N_{l,2^j} = N_{l-1,j} - N_{l,2^j-1}$. Denoting $\vec{N}_{l,*} = (N_{l,1}, \dots, N_{l,2^l})$, recursively invoking these relations we may express,

$$\begin{aligned}
\Pr(\vec{N}_{L,*}|\vec{d}) &= \Pr(\vec{N}_{1,*}, \dots, \vec{N}_{L,*}|\vec{d}) \\
&= \Pr(\vec{N}_{L,*}|\vec{N}_{1,*}, \dots, \vec{N}_{L-1,*}, \vec{d}) \cdot \Pr(\vec{N}_{1,*}, \dots, \vec{N}_{L-1,*}|\vec{d}) \\
&= \Pr(\vec{N}_{L,*}|\vec{N}_{L-1,*}, \vec{d}) \cdot \Pr(\vec{N}_{L-1,*}|\vec{N}_{1,*}, \dots, \vec{N}_{L-2,*}, \vec{d}) \cdot \Pr(\vec{N}_{1,*}, \dots, \vec{N}_{L-2,*}|\vec{d}) \\
&= \Pr(\vec{N}_{L,*}|\vec{N}_{L-1,*}, \vec{d}) \cdot \Pr(\vec{N}_{L-1,*}|\vec{N}_{L-2,*}, \vec{d}) \cdots \Pr(\vec{N}_{2,*}|\vec{N}_{1,*}, \vec{d}) \cdot \Pr(\vec{N}_{1,*}|\vec{d}). \tag{4}
\end{aligned}$$

Now that we have derived $\Pr(\vec{d}|\vec{u})$, we express the conditional distribution of $\vec{\phi}$,

$$f(\vec{\phi}|\vec{u}) = \sum_{\vec{d} \in \mathcal{D}} f(\vec{\phi}, \vec{d}|\vec{u}) = \sum_{\vec{d} \in \mathcal{D}} f(\vec{\phi}|\vec{d}, \vec{u}) \cdot \Pr(\vec{d}|\vec{u}), \tag{5}$$

where $f(\vec{\phi}|\vec{d}, \vec{u})$ is the conjugate posterior density of $\vec{\phi}$ given \vec{d} and \vec{u} for the hBeta model.

Example 2.3 According to Expression (2), the conditional segmentation probability, $\Pr(\vec{d}|\vec{u})$, is proportional to the product of the reciprocal of the multinomial coefficient for the counts vector $\vec{N}_{L,*}$ in (3) and the conditional probability of the counts vector, $\Pr(\vec{N}_{L,*}|\vec{d})$, which is determined by a_0 .

Recall that in Model 2.1 given $\vec{\pi}_L$ and \vec{d} , $\vec{N}_{L,*}$ is multinomial with sample size m and probabilities vector $\vec{\pi}_L$. Thus the results of Example 2.2 suggest that for small values of a_0 large probabilities will be given to unevenly distributed counts vectors and that increasing a_0 will favour more evenly distributed counts vectors.

To illustrate the effect of a_0 on $\Pr(\vec{d}|\vec{u})$, in Table 1 we list conditional segmentation probabilities for a set of $L = 2$ level segmentations, $\mathcal{D} = \{\vec{d}_1, \dots, \vec{d}_5\}$, and a sample of $m = 4$ observations, $\vec{u} = (u_1, \dots, u_4)$, in the unit cube $[0, 1]^P$. The rows of Table 1 correspond to the segmentations, $\vec{d}_1 \cdots \vec{d}_5$. The counts

vector, $\vec{N}_{2,*}(\vec{u}; \vec{d}_j) = (N_{2,1}, \dots, N_{2,4})$, for \vec{d}_j is listed in Column 1. In columns 2-4, we list $\Pr(\vec{d}_j|\vec{u})$ for $a_0 = 0.1, 1, 10$.

Indeed, we see that increasing a_0 provides larger probabilities to the segmentations that yield more evenly distributed count vectors at the first rows of Table 1. Furthermore, comparing the second and third rows reveals that the segmentation probabilities is not exchangeable in $\vec{N}_{2,*}$, where for each value of a_0 , segmentations that yield contiguous non-zero counts are more probable. Yet, the two segmentations yielding counts vector with a single non-zero entry are equally probable.

$\vec{N}_{2,*}(\vec{u}; \vec{d}_j)$	$a_0 = 0.1$	$a_0 = 1$	$a_0 = 10$
(1, 1, 1, 1)	0.00	0.01	0.13
(0, 2, 0, 2)	0.00	0.04	0.16
(0, 0, 2, 2)	0.01	0.07	0.19
(0, 0, 0, 4)	0.49	0.44	0.26
(0, 0, 4, 0)	0.49	0.44	0.26

Table 1: Conditional segmentation probabilities.

2.4 Predictive inference

The predictive distribution is the distribution of u_{m+1} for generative model 2.1. Let $f(u)$ denote the density function for the predictive distribution, which is a mixture of $f(u|\vec{d}, \vec{\phi})$ for random $\vec{d} \in \mathcal{D}$ and $\vec{\phi}$. The predictive probability of $\mathcal{U} \subset [0, 1]^P$ is given by

$$\Pr(u_{m+1} \in \mathcal{U}) = \int_{u \in \mathcal{U}} f(u) du. \quad (6)$$

Let \mathcal{U}' be a sufficiently small subset, so that $\forall \vec{d} \in \mathcal{D}$ it is a subset of a single level L subinterval. As $f(u|\vec{d}, \vec{\phi})$ is constant on \mathcal{U}' for all \vec{d} , then $f(u)$ is constant on \mathcal{U}' and therefore

$$\Pr(u_{m+1} \in \mathcal{U}') = \text{volume}(\mathcal{U}') \cdot f(u).$$

And in general, $f(u)$ is piecewise constant.

For $l = 1 \dots L$, let $j'(l, \vec{d})$ denote the index of the l level subinterval for segmentation $\vec{d} \in \mathcal{D}$ that covers \mathcal{U}' . Per construction $\forall \vec{d} \in \mathcal{D}$ and $\forall u \in \mathcal{I}_{L, j'(L, \vec{d})}(\vec{d})$,

$$f(u|\vec{d}, \vec{\phi}) = 2^L \cdot \pi_{L, j'(L, \vec{d})}(\vec{d}),$$

for $\pi_{L, j'(L, \vec{d})}$ that is a product of $\phi_{1, j'(1, \vec{d})} \dots \phi_{L, j'(L, \vec{d})}$. Therefore given \vec{d} and $\vec{\phi}$, we may express the conditional predictive probability of \mathcal{U}' ,

$$\Pr(u_{m+1} \in \mathcal{U}'|\vec{d}, \vec{\phi}) = \text{volume}(\mathcal{U}') \cdot 2^L \cdot \prod_{l=1}^L \phi_{j, j'(j, \vec{d})}(\vec{d}). \quad (7)$$

As any Bayesian model, our inferential framework provides Bayesian estimates and credible regions for the model parameters. For predictive inference we further consider three types of outcomes:

a. Predictive samples. Predictive samples, $u_{m+1}^1 \dots u_{m+1}^n$, are iid samples from the predictive distribution. Predictive samples may be generated by repeating the following steps for $i = 1 \dots n$: Sample $(\vec{d}, \vec{\phi}(\vec{d}))$, compute $\bar{\pi}_L(\vec{d})$, sample $u_{m+1}^i \sim f(u|\vec{d}, \bar{\pi}_L(\vec{d}))$.

b. Predictive probabilities. The predictive probability of \mathcal{U} is $\Pr(u_{m+1} \in \mathcal{U})$ for generative model 2.1. This outcome may be numerically evaluated by computing the proportion of predictive samples in \mathcal{U} ,

$$\Pr(u_{m+1} \in \mathcal{U}) \hat{=} \frac{|(i : u_{m+1}^i \in \mathcal{U})|}{n}.$$

In the next two subsections we analytically derive the predictive probability of \mathcal{U}' .

c. Credible prediction sets. A level $1 - \alpha$ credible prediction set is $\mathcal{U}_{1-\alpha} \subset [0, 1]^P$ with predictive probability $1 - \alpha$. Thus the number predictive samples in $\mathcal{U}_{1-\alpha}$ is a *Binomial*($n, 1 - \alpha$) random variable.

2.4.1 The prior predictive distribution

The prior predictive distribution is the marginal distribution of u_{m+1} in generative model 2.1, in which \vec{d} is sampled from \mathcal{D} with equal probabilities and $\phi_{l,j}(\vec{d})$ are iid *Beta*(a_0, a_0). Thus using (7) we may express the predictive probability of \mathcal{U}' ,

$$\begin{aligned} \Pr(u_{m+1} \in \mathcal{U}') &= E_{\vec{\phi}, \vec{d}} \left[\Pr(u_{m+1} \in \mathcal{U}' | \vec{d}, \vec{\phi}) \right] = E_{\vec{\phi}, \vec{d}} \left[\text{volume}(\mathcal{U}') \cdot 2^L \cdot \prod_{l=1}^L \phi_{j,j'(l,\vec{d})}(\vec{d}) \right] \\ &= \text{volume}(\mathcal{U}') \cdot 2^L \cdot E_{\vec{d}} \prod_{l=1}^L E_{\vec{\phi} | \vec{d}} \left[\phi_{l,j'(j,\vec{d})}(\vec{d}) \right] = \text{volume}(\mathcal{U}') \cdot 2^L \cdot \prod_{l=1}^L \left(\frac{a_0}{a_0 + a_0} \right) \\ &= \text{volume}(\mathcal{U}'). \end{aligned} \quad (8)$$

Therefore the prior predictive distribution is the uniform distribution with $f(u) \equiv 1$.

2.4.2 The posterior predictive distribution

The posterior predictive distribution of u_{m+1} is the conditional distribution of u_{m+1} given $\vec{u} = (u_1 \cdots u_m)$ in generative model 2.1.

Conditional on \vec{d} and on $\vec{N} = \vec{N}_{L,*}(\vec{u}; \vec{d})$, $\pi_{L,j'(l,\vec{d})} = \prod_{l=1}^L \phi_{l,j'(l,\vec{d})}$, with independent $\phi_{1,j'(1,\vec{d})} \sim \text{Beta}(a_0 + N_{1,j'(1,\vec{d})}, a_0 + m - N_{1,j'(1,\vec{d})})$ and $\phi_{l,j'(l,\vec{d})} \sim \text{Beta}(a_0 + N_{l,j'(l,\vec{d})}, a_0 + N_{l-1,j'(l-1,\vec{d})} - N_{l,j'(l,\vec{d})})$ for $l = 2 \cdots L$. Thus using (7) we may express

$$\begin{aligned} \Pr(u_{m+1} \in \mathcal{U}' | \vec{N}, \vec{d}) &= E_{\vec{\phi} | \vec{N}, \vec{d}} \left[\Pr(u_{m+1} \in \mathcal{U}' | \vec{d}, \vec{\phi}) \right] \\ &= \text{volume}(\mathcal{U}') \cdot 2^L \cdot \prod_{l=1}^L E_{\vec{\phi} | \vec{N}, \vec{d}} \left[\phi_{l,j'(l,\vec{d})}(\vec{d}) \right] \\ &= \text{volume}(\mathcal{U}') \cdot 2^L \cdot \left[\prod_{l=1}^L \left(\frac{N_{l,j'(l,\vec{d})} + a_0}{N_{l-1,j'(l-1,\vec{d})} + 2 \cdot a_0} \right) \right], \end{aligned} \quad (9)$$

with $N_{0,j'(0,\vec{d})} = m$. Recalling that the sequence subinterval counts is decreasing, $m \geq N_{1,j'(1,\vec{d})} \geq \cdots \geq N_{L,j'(L,\vec{d})}$, let L' denote the largest l with a nonzero count, i.e. $N_{L',j'(L',\vec{d})} > 0$. Therefore we may rewrite Expression (9),

$$\begin{aligned} &\Pr(u_{m+1} \in \mathcal{U}' | \vec{N}, \vec{d}) \\ &= \text{volume}(\mathcal{U}') \cdot 2^L \cdot \frac{N_{1,j'(1,\vec{d})} + a_0}{m + 2a_0} \cdot \frac{N_{2,j'(2,\vec{d})} + a_0}{N_{1,j'(1,\vec{d})} + 2a_0} \cdots \frac{N_{L',j'(L',\vec{d})} + a_0}{N_{L'-1,j'(L'-1,\vec{d})} + 2a_0} \cdot \left(\frac{a_0}{2a_0} \right)^{L-L'} \\ &= \text{volume}(\mathcal{U}') \cdot 2^{L'} \cdot \frac{N_{1,j'(1,\vec{d})} + a_0}{m + 2a_0} \cdot \frac{N_{2,j'(2,\vec{d})} + a_0}{N_{1,j'(1,\vec{d})} + 2a_0} \cdots \frac{N_{L',j'(L',\vec{d})} + a_0}{N_{L'-1,j'(L'-1,\vec{d})} + 2a_0}, \end{aligned} \quad (10)$$

and thus for $u \in \mathcal{U}'$ the conditional posterior predictive density is

$$f(u|\vec{N}, \vec{d}) = 2^{L'} \cdot \frac{N_{1,j'(1,\vec{d})} + a_0}{m + 2a_0} \cdot \frac{N_{2,j'(2,\vec{d})} + a_0}{N_{1,j'(1,\vec{d})} + 2a_0} \cdot \dots \cdot \frac{N_{L',j'(L',\vec{d})} + a_0}{N_{L'-1,j'(L'-1,\vec{d})} + 2a_0}. \quad (11)$$

Note that for $a_0 \rightarrow 0$, the numerator in the l 'th term and the denominator of the $l + 1$ 'th term in the product in (11) are equal for $l = 1 \dots L' - 1$, thereby yielding

$$\lim_{a_0 \rightarrow 0} f(u|\vec{N}, \vec{d}) = 2^{L'} \cdot \frac{N_{L',j'(L',\vec{d})}}{m}. \quad (12)$$

On the other hand, increasing a_0 shrinks each of the L' fraction terms in (11) to $1/2$, yielding

$$\lim_{a_0 \rightarrow \infty} f(u|\vec{N}, \vec{d}) = 2^{L'} \cdot (1/2)^{-L'} = 1. \quad (13)$$

Lastly, the posterior predictive probability of \mathcal{U}' is a mixture of the conditional posterior predictive probabilities in (10),

$$\Pr(u_{m+1} \in \mathcal{U}'|\vec{u}) = \sum_{\vec{d} \in \mathcal{D}} \Pr(u_{m+1} \in \mathcal{U}', \vec{d}|\vec{u}) = \sum_{\vec{d} \in \mathcal{D}} \Pr(u_{m+1} \in \mathcal{U}'|\vec{N}(\vec{u}; \vec{d}), \vec{d}) \cdot \Pr(\vec{d}|\vec{u}), \quad (14)$$

where $\Pr(\vec{d}|\vec{u})$ is the posterior segmentation probability in (2). And the posterior predictive density for $u \in \mathcal{U}'$ is a mixture of the conditional densities in (11),

$$f(u|\vec{u}) = \frac{\Pr(u_{m+1} \in \mathcal{U}'|\vec{u})}{\text{volume}(\mathcal{U}')} = \sum_{\vec{d} \in \mathcal{D}} f(u|\vec{N}(\vec{u}; \vec{d}), \vec{d}) \cdot \Pr(\vec{d}|\vec{u}).$$

2.5 Frequentist properties of our inferential framework

Recall, the underlying assumption in this report is that the real data generative model is that $u_1 \dots u_{m+1}$ are iid $\tilde{\pi}$. We will use subscript $\tilde{\pi}$ to denote real probabilities, all other probability statements are with respect to model 2.1.

We begin by considering a single segmentation \vec{d} . Let $\tilde{\pi}_L(\vec{d}) = (\tilde{\pi}_{L,1}, \dots, \tilde{\pi}_{L,2^L})$ denote the vector of probabilities that $\tilde{\pi}$ assigns to subintervals $\mathcal{I}_{L,1}(\vec{d}), \dots, \mathcal{I}_{L,2^L}(\vec{d})$. Thus the real sampling distribution of $\vec{N} = \vec{N}_{L,*}(\vec{u}; \vec{d})$ is Multinomial with number of trials m and event probabilities vector $\tilde{\pi}_L(\vec{d})$. In our inferential framework, the real probability that $u_{m+1} \in \mathcal{U}'$ is estimated by the conditional posterior predictive probability

$$\Pr_{\tilde{\pi}}(u_{m+1} \in \mathcal{U}') \hat{=} \Pr(u_{m+1} \in \mathcal{U}'|\vec{N}, \vec{d}) = \text{volume}(\mathcal{U}') \cdot f(u|\vec{d}, \vec{N}).$$

To assess how well we evaluate $\tilde{\pi}$ with a given segmentation \vec{d} , we consider two types of errors: (a) approximation error, defined as the distance between $\tilde{\pi}$ and step-function density

$$f(u; \vec{d}, \tilde{\pi}_L) = \tilde{\pi}_{L,1} \cdot \frac{I_{L,1}(u; \vec{d})}{(1/2)^L} + \dots + \tilde{\pi}_{L,2^L} \cdot \frac{I_{L,2^L}(u; \vec{d})}{(1/2)^L}, \quad (15)$$

which is an irreducible term that depends on the smoothness of $\tilde{\pi}$ with respect to \vec{d} ; (b) estimation error of $f(u; \vec{d}, \tilde{\pi}_L)$ by $f(u|\vec{d}, \vec{N})$, which is reduced by increasing m . The estimation error may be further divided into bias and variance terms.

In general, coarse segmentations have large approximation error and small estimation error. Refining the segmentation by increasing L , decreases the approximation error and increases the estimation error. For coarse segmentation \vec{d} and sufficiently large m that ensures that $N_{L,j'(L,\vec{d})} > 0$ and thus $L' = L$, Expression (12) implies that for $u \in \mathcal{U}'$,

$$\begin{aligned} E_{u_1 \dots u_m \sim \tilde{\pi}} \lim_{a_0 \rightarrow 0} f(u|\vec{d}, \vec{N}) &= E_{\tilde{\pi}} \frac{2^L \cdot N_{L,j'(L,\vec{d})}(\vec{d})}{m} = \frac{E_{\tilde{\pi}} N_{L,j'(L,\vec{d})}(\vec{d})}{(1/2)^L \cdot m} \\ &= \frac{m \cdot \tilde{\pi}_{L,j'(L,\vec{d})}}{(1/2)^L \cdot m} = f(u; \vec{d}, \tilde{\pi}_L). \end{aligned}$$

Therefore for small a_0 and coarse segmentations $f(u|\vec{d}, \vec{N})$ has small bias.

On the other hand, if $L' < L$ then according to Expression (11), $f(u|\vec{d}, \vec{N}) = f(u|\vec{d}', \vec{N})$ for any segmentation \vec{d}' that is a refinement of \vec{d} . As a result, our density estimators maintain small estimation error for fine segmentations. This is especially useful for larger values of a_0 that yield biased density estimation with small estimation variance. According to the simulations in Subsection 3.1, setting $a_0 = 1$ provide small estimation error even for fine segmentations and small m .

Our inferential framework considers multiple segmentations \vec{d} , with different approximation and estimation errors, that are weighted according to the posterior segmentation probability $\Pr(\vec{d}|\vec{u})$. The most interesting and surprising feature of our framework is that for $a_0 = 1$ segmentations with large posterior probabilities tend to have small approximation and estimation errors. We will demonstrate this in simulations in Subsection 3.2.

Our inferential framework also produces level $1 - \alpha$ credible prediction sets, $\mathcal{U}_{1-\alpha} \subset [0, 1]^P$. Per construction, credible prediction sets have posterior predictive probability $1 - \alpha$, $\Pr(u_{m+1} \in \mathcal{U}_{1-\alpha}|\vec{u}) = 1 - \alpha$. In Section 4, we will demonstrate how our inferential framework may be adapted to produce conformal prediction sets $\tilde{\mathcal{U}}_{1-\alpha} \subset [0, 1]^P$, for which $\Pr_{\tilde{\pi}}(u_{m+1} \in \tilde{\mathcal{U}}_{1-\alpha}) \geq 1 - \alpha$.

3 Density estimation simulations

3.1 Simulation study of 1D density estimation

In this subsection we present the results of simulations studying the performance of our density estimators for estimating $\tilde{\pi}$ that has a piecewise continuous density on $[0, 1]$. In each simulation run we generate a sample of iid observations $\vec{u} = (u_1, \dots, u_m)$ from $\tilde{\pi}$ and use it to compute $f(u|\vec{d}, \vec{N})$ for $L = 10, 5, 3$, and a set value of a_0 . As we estimate a $P = 1$ dimensional density, we consider the canonical segmentation of $\mathcal{I}_0 = [0, 1]$, in which $\mathcal{I}_{l,j} = [(j-1) \cdot 2^{-l}, j \cdot 2^{-l}]$ for $l = 1 \dots L$ and $j = 1 \dots 2^l$. We performed 4 sets of simulations with $m = 50, 200$ and $a_0 = 1, 0.1$, each consisting of 10,000 simulation runs.

The simulation results are presented in Figure 4. Each pair of plots corresponds to the same set of simulations: the left plot displays the simulation mean of $f(u|\vec{d}, \vec{N})$; the right plot displays the square root of the simulation mean of the estimator squared-error, $(\hat{\pi}(u) - \tilde{\pi}(u))^2$, for $\hat{\pi}(u) = f(u|\vec{d}, \vec{N})$ and for the interval-counts density estimators, $\hat{\pi}(u) = 2^L \cdot N_{L,j}(\vec{u}; \vec{d})/m$. The black curve in all the plots is $\tilde{\pi}(u)$, the piecewise continuous density we are estimating. The green, blue, red curves correspond to level $L = 10, 5, 3$, segmentations of $[0, 1]$. Solid curves are drawn for the hBeta estimators and dashed curves are drawn for the interval-counts estimators.

The estimator mean plots reveal estimation bias and approximation error. For $m = 50$ and $a_0 = 1$ the hBeta density estimators are biased – upward bias for small density values and downward bias for large density values. For $m = 200$ and $a_0 = 1$ the bias of the estimators is smaller. For $a_0 = 0.1$ the

bias is considerably smaller and can only be observed for the small density values. The bias does seem to depend on L .

To assess approximation errors, which do not depend on m and a_0 , we focus on the $m = 200$ and $a_0 = 0.1$ configuration that has the smallest bias. There is no approximation error in the regions in which $\tilde{\pi}(u)$ is constant. In the region in which $\tilde{\pi}(u)$ is linear in u , there is considerable approximation for $L = 3$ that decreases as L increases.

The estimator MSE is the sum of the squared estimation error and the squared approximation error. In this example the estimation error is considerably larger than the approximation error. The hBeta estimator MSE decreases in m , and given m and a_0 it increases in L . For $L = 3$, $m = 200$ and $a_0 = 0.1$, the MSE of the hBeta estimator is the same as the MSE of the interval-counts estimator, which is unbiased with $MSE = (2^L)^2 \cdot \tilde{\pi}(u) \cdot (1 - \tilde{\pi}(u)) / m$ for all L and m . The ratio between the MSE of the interval-counts estimator and the hBeta estimator increases for larger L and a_0 and smaller m . For $L = 10$, $m = 50$ and $a_0 = 1$, the sqrt(MSE) of the hBeta estimator is 4 – 5 times smaller than that of the interval-counts estimator.

3.2 Simulation study of 2D density estimation

In this subsection, for $u = (u_x, u_y)$, we present simulation results for estimating $\tilde{\pi}(u) = 2 \cdot \text{logit}^{-1}(20 \cdot (u_x - 0.5))$ with $f(u|\vec{d}, \vec{N})$, for the four $L = 4$ level segmentations of $[0, 1]^2$ shown in Figure 1.

The results are displayed in Figure 5. In the top row of plots we show how well $\tilde{\pi}$ is approximated by $f(u; \vec{d}, \tilde{\pi}_L)$ in the the four segmentations of $[0, 1]^2$. In each plot, the regions separated by the green vertical lines in each plot correspond to the 16 subintervals of each segmentation, $\mathcal{I}_{4,1}(\vec{d}) \cdots \mathcal{I}_{4,16}(\vec{d})$, arranged from left to right. Thus, in the four plots the last interval on the right is $\mathcal{I}_{4,16}(\vec{d})$. According to Figure 1, for segmentation (X, X, X, X) , $\mathcal{I}_{4,16}(\vec{d})$ is the subinterval on the right end of $[0, 1]^2$; for segmentation (Y, Y, Y, Y) , $\mathcal{I}_{4,16}(\vec{d})$, is the subinterval on the top end of $[0, 1]^2$; for segmentations (X, X, Y, Y) and (Y, Y, X, X) , $\mathcal{I}_{4,16}(\vec{d})$ is the subinterval on the top right corner of $[0, 1]^2$.

In the four plots, the black curves display the profile of $\tilde{\pi}(u)$ as a function of u_x and the red horizontal lines display $f(u; \vec{d}, \tilde{\pi}_L)$, for each subinterval. We summarize the approximation error for each segmentation by the square root of a MSE measuring the distance between $\tilde{\pi}(u)$ and $f(u; \vec{d}, \tilde{\pi}_L)$,

$$MSE\left(\tilde{\pi}(u), f(u; \vec{d}, \tilde{\pi}_L)\right) := \int_{u \in [0, 1]^2} \left(\tilde{\pi}(u) - f(u; \vec{d}, \tilde{\pi}_L)\right)^2 du = \sum_{j=1}^{16} \int_{u \in \mathcal{I}_{4,j}(\vec{d})} \left(\tilde{\pi}(u) - \tilde{\pi}_{L,j}(\vec{d})\right)^2 du.$$

Segmentation (X, X, X, X) has the smallest approximation error, $\text{sqrt}(MSE) = 0.066$; Segmentation (Y, Y, Y, Y) has the largest approximation error, $\text{sqrt}(MSE) = 0.894$; the approximation error for segmentations (X, X, Y, Y) and (Y, Y, X, X) , that have the same set level $L = 4$ subintervals, is $\text{sqrt}(MSE) = 0.199$;

The simulation study consisted of 10,000 simulation runs. In each run, $m = 50$ iid $u_i \sim \tilde{\pi}(u)$ were generated and used to compute $\Pr(\vec{d}|\vec{u})$ and the hBeta estimator, $\hat{\pi}_{L,j}(\vec{N}; \vec{d}) = \Pr(u_{m+1} \in \mathcal{I}_{L,j}(\vec{d})|\vec{N}, \vec{d})$, for each segmentation with $a_0 = 1$. The estimation error of $\hat{\pi}_{L,j}(\vec{N}; \vec{d})$ is summarized by the Pearson residual, $(\hat{\pi}_{L,j}(\vec{N}; \vec{d}) - \tilde{\pi}_{L,j}(\vec{d})) / \sqrt{\tilde{\pi}_{L,j}(\vec{d})}$. Note that for each simulation run $\vec{N} \sim \text{Multinomial}(50; \tilde{\pi}_L(\vec{d}))$. Therefore Pearson residual for the counts estimator, $\hat{\pi}_{L,j}(\vec{N}; \vec{d}) = N_{L,j}(\vec{d})/50$, is approximately $N(0, 1)$ and the resulting X^2 statistic, which is the sum of squares of the 16 Pearson residuals, is a chi-square random variable with 15 degrees of freedom.

The boxplots in the bottom row of Figure 5 display the distribution of the simulation outcomes. The left and middle sets of boxplots display the distribution of X^2 and the distribution of the mean

of the absolute value of the Pearson residuals, for the four segmentations. The plots reveal that the estimation error for all four segmentations is considerably smaller than the estimation error for the counts estimator, for which the expectation of the X^2 statistic is 15 and the expectation of the mean of the absolute value of the Pearson residual is approximately $E_{Z \sim N(0,1)}|Z| = 0.798$. As our estimation algorithm shrinks the density at each level to the Uniform density, the estimation error is minimized for segmentation (Y, Y, Y, Y) for which the 16 estimated probabilities are equal, and increases as the differences in probabilities between contiguous subinterval increase. Thus even though the set of estimated probabilities is the same for segmentations (X, X, Y, Y) and (Y, Y, X, X) , the estimation error is much smaller for segmentation (X, X, Y, Y) for which the set of probabilities is ordered.

The four boxplots on the right display the distribution of posterior segmentation probability $\Pr(\vec{d}|\vec{u})$ for each segmentation. The plots reveal that (X, X, X, X) that has the smallest approximation error is the most probable segmentation. Segmentation (Y, Y, Y, Y) that has the largest approximation error has almost 0 posterior probability. Of the two segmentations with the same approximation error, segmentation (X, X, Y, Y) that has the smaller estimation error has considerably larger posterior probabilities.

4 Quantile regression simulation

In this simulated example $\tilde{\pi}(u)$ is the density of $U = (U_x, U_y)$, where $U_x = \text{logit}^{-1}(X)$ for $X \sim N(0, 4)$, and $U_y = \text{logit}^{-1}(Y)$ with $Y|X = x \sim N(-0.9, 0.25)$ for $x < -1$ and $Y|X = x \sim N(0.9 \cdot x, 0.25)$ for $x \geq -1$. We segment $\mathcal{I}_0 = [0, 1]^2$ with $L = 8$ dyadic segmentations. Similarly to the previous 2D example, we only consider \vec{d} in which all the subintervals at the same level are partitioned according to the same dimension. In this case \mathcal{D} is the set of $70 = \binom{8}{4}$ segmentations consisting of four X partitions and four Y partitions that produce an array of 16×16 square subintervals, and we set $a_0 = 1$.

The plots in Figure 6 correspond to simulations with sample size $m = 100$ (top) and $m = 1000$ (bottom). In each plot, the red X's mark the observations, $u_1 \cdots u_m$, and the blue curves are the 0.05, 0.50 and 0.95 quantiles of $\tilde{\pi}(U_y|U_x = u_x)$. Per construction, for all $u_x \in [0, 1]$ the interval between the dashed blue lines forms a 0.90 conditional predictive interval for $U_y \sim \tilde{\pi}(U_y|U_x = u_x)$. Thus the region between the dashed blue lines is a 0.90 predictive set for $U \sim \tilde{\pi}$.

In order to produce predictive inferences, for each segmentation $\vec{d}_j \in \mathcal{D}$, we compute the posterior segmentation probability $\Pr(\vec{d}_j|\vec{u})$, and generate 50 Beta vectors from the conditional distribution of $\vec{\phi}$ given \vec{d}_j and $\vec{N}(\vec{u}; \vec{d}_j)$ and use them to compute probability vectors, $\vec{\pi}_L^{j,1} \cdots \vec{\pi}_L^{j,50}$. We approximate the posterior predictive density $f(u|\vec{u})$ by the mixture density

$$\sum_{j=1}^{70} \sum_{h=1}^{50} \frac{\Pr(\vec{d}_j|\vec{u})}{50} f(u|\vec{\pi}_L^{j,h}, \vec{d}_j). \quad (16)$$

The Green circles in each plot, are 2000 posterior predictive samples, $u_{m+1}^1 \cdots u_{m+1}^{2000}$, drawn independently from mixture density (16). The Orange curves are the 0.05, 0.50 and 0.95 quantiles of the conditional distribution of U_y given $U_x = u_x$ for mixture density (16). Note that as the mixture density is piecewise constant on an array of 16×16 subintervals, each quantile profile is piecewise constant on the 16 subintervals of U_x . For all $u_x \in [0, 1]$ the interval between the dashed Orange lines form a 0.90 conditional posterior predictive interval for $U_y|U_x = u_x$, thus the region between the dashed lines is a 0.90 posterior credible prediction set.

The plots reveal that the posterior predictive density captures the general shape of $\tilde{\pi}$ pretty well. For $m = 100$, the conditional posterior predictive distribution is more spread out than $\tilde{\pi}(U_y|U_x = u_x)$, especially for values of u_x close to 1, for which $\tilde{\pi}(U_y|U_x = u_x)$ converges to 1. For $m = 1000$, the distribution of the posterior predictive samples is more similar to the distribution of $u_1 \cdots u_m$, and other than an approximation error, the quantiles of the conditional posterior predictive distribution and the quantiles of $\tilde{\pi}(U_y|U_x = u_x)$ are almost the same for all u_x .

4.1 Conformal Prediction sets

Vovk et al. (2005) present a general algorithm for constructing prediction sets for the following setting: $w_1 \cdots w_{m+1}$ are iid $\tilde{\pi}(w)$, with $w_i = (x_i, y_i)$. On observing the training set $\{w_1 \cdots w_m\}$ and x_{m+1} , the goal is to construct a prediction set for y_{m+1} . The key component for constructing the prediction sets is the conformity score, $A(\{w_1 \cdots w_m\}, w) \in \mathbb{R}$, that shows how well an additional point $w = (x, y)$ conforms to the training set. They prove that Conformal Prediction Sets constructed in Algorithm 4.1 cover y_{m+1} with probability $\geq 1 - \alpha$.

Definition 4.1 Algorithm for constructing Conformal Prediction Sets

1. For each potential value y of y_{m+1} , compute the conformity score

$$a_{m+1}(y) = A(\{w_1, \dots, w_m\}, (x_{m+1}, y)).$$

To assess the significance of $a_{m+1}(y)$, for $i = 1 \cdots m$ compute conformity score

$$a_i(y) = A(\{w_1, \dots, w_{i-1}, (x_{m+1}, y), w_{i+1}, \dots, w_m\}, w_i),$$

and compute the rank-based p-value

$$p(y) = \frac{|\{i : a_i(y) \leq a_{m+1}(y)\}|}{m+1}.$$

2. The $1 - \alpha$ Conformal Prediction Set for y_{m+1} is then defined

$$\tilde{\mathcal{Y}}_{1-\alpha} := \{y : p(y) > \alpha\}.$$

To construct conformal prediction sets for the quantile regression example, we define the conformity score between training set \vec{u} and an additional point $u_{m+1} = (u_x, u_y)$ to be the conditional posterior predictive given \vec{u} and $U_x = u_x$ that $U_y \leq u_y$,

$$A(\vec{u}, u) := \Pr(U_y \leq u_y | U_x = u_x, \vec{u}). \quad (17)$$

To apply Algorithm 4.1, $a_{m+1}(y)$ is conformity score (17) for $u_{m+1} = (u_x, u_y)$ and training set $\{u_1 \cdots u_m\}$, which we numerically evaluate with mixture density (16). However for $i = 1 \cdots m$, $a_i(y)$ is conformity score (17) for $u_{m+1} = u_i$ and training set $\vec{u}^{(i)} \cup \{u_{m+1}\}$, with $\vec{u}^{(i)} = \{u_1, \dots, u_{i-1}, u_{i+1}, \dots, u_m\}$. We evaluate $a_i(y)$ by generating a mixture density (16) that approximates posterior predictive density $f(u | \vec{u}^{(i)} \cup \{u_{m+1}\})$.

Note that for $m \rightarrow \infty$ the posterior predictive distribution $f(u | \vec{u})$ identifies with $\tilde{\pi}(u)$, in which case the conformity score in (17) for $u \sim \tilde{\pi}(u)$ is a $U[0, 1]$ random variable and thus the conformity score identifies with its significance level in Algorithm 4.1, $a_{m+1}(y) = p(y)$. Thereby implying that the bottom end of the $1 - \alpha$ Conformal Prediction Set for y_{m+1} is the α quantile of the conditional posterior predictive distribution of $U_y | U_x = u_x$.

In the top row of Figure 7 we present $U[0, 1]$ qqplots for the sequence of conformity scores, between each of the m observations and the training set consisting of the remaining $m - 1$ observation, for the simulated examples shown in figure 6. For $m = 1000$, we see that the distribution of the conformity scores for the observations is very close to $U[0, 1]$. Thus the ends of the 0.90 Conformal Prediction sets would be very close to the dashed orange curves in the bottom plot in Figure 6.

In the bottom of figure 7, we display the Conformal Prediction sets for the $m = 100$ simulated example in Figure 6. The lower purple dashed curve marks the bottom ends of the 0.95 Conformal Prediction Sets for y_{m+1} for all $u_x \in [0, 1]$, for conformity score $\Pr(U_y \leq u_y | U_x = u_x, \vec{u})$. The upper purple dashed curve marks the top ends of the 0.95 Conformal Prediction Sets for y_{m+1} for all $u_x \in [0, 1]$, for conformity score $\Pr(U_y \geq u_y | U_x = u_x, \vec{u})$. Thus the region between the two purple curves forms a 0.95 Conformal Prediction Set for u_{m+1} .

5 High Dimensional Predictive Inference simulation

In this section, $\tilde{\pi}$ is the joint distribution of a categorical variable X , which takes on values “a”, “b”, “c” with probabilities 0.5, 0.3, 0.2, and a continuous 8-dimensional random vector $\vec{Y} = (Y_1 \cdots Y_8)$, with conditional distribution $\vec{Y}|X = x \sim N(\vec{\mu}_x, \Sigma_x)$. $\vec{\mu}_x = (0, \dots, 0)'$ and or all values of X ; for $X = b$ or $X = c$, $\Sigma_x = I_{8 \times 8}$; for $X = a$, $\text{cov}(Y_1, Y_2) = 0.8$, other than that $\Sigma_x = I_{8 \times 8}$.

In the simulated example, we generate $m = 400$ iid realizations of $\tilde{\pi}(x, \vec{y})$, $(x_i, \vec{y}_i) = (x_i, y_{i,1}, \dots, y_{i,8})$ for $i = 1 \cdots m$. Our goal is to produce $n = 1000$ posterior predictive samples, $(x_{m+1}^1, \vec{y}_{m+1}^1), \dots, (x_{m+1}^n, \vec{y}_{m+1}^n)$.

To apply our methodology, for $i = 1 \cdots m$ (x_i, \vec{y}_i) is transformed to $\vec{u}_i = (u_{i,1} \cdots u_{i,10})$ as follows. For $j = 1 \cdots 8$, the support of continuous variable Y_j is inflated by 2% and partitioned into 16 subintervals. For $l = 0 \cdots 16$, let $q_{l,j}$ denote the $l/16$ quantile of $(y_{1,j}, \dots, y_{m,j})$. The marginal subintervals are then defined: $I_1^j = [q_{0,j} - (q_{16,j} - q_{0,j})/100, q_{1,j}]$, $I_l^j = [q_{l-1,j}, q_{l,j}]$ for $l = 2 \cdots 15$, $I_{16}^j = [q_{15,j}, q_{16,j} + (q_{16,j} - q_{0,j})/100]$. For $i = 1 \cdots m$, we set $u_{i,j} = 1/32 + (l-1)/16$ for $y_{i,j} \in I_l^j$. Thus $u_{1,j} \cdots u_{m,j}$ take on the values $\{\frac{1}{32}, \frac{3}{32}, \dots, \frac{31}{32}\}$ with probabilities 1/16. The categorical variable x_i is encoded by two dichotomous variables: $u_{i,9} = 1/4$ for $x_i \neq b$ and $u_{i,9} = 3/4$ for $x_{i,9} = b$; $u_{i,10} = 1/4$ for $x_i \neq c$ and $u_{i,10} = 3/4$ for $x_{i,9} = c$.

The sample $\vec{u}_1 \cdots \vec{u}_m$ is segmented with $L = 10$ dyadic segmentations of $[0, 1]^{10}$, where for $j = 1 \cdots 8$ variable U_j may be segmented 4 times in halve and for $j = 9, 10$ variable U_j may be segmented in halve once. \mathcal{D} is the set of $1960 = \binom{8}{4} \cdot \binom{8}{2}$ segmentations, in which $[0, 1]^{10}$ is first partitioned according to U_{10} and U_9 and then according to either U_{j_1} or U_{j_2} – four partitions in each dimension – for all $j_1 \neq j_2$ in $\{1 \cdots 8\}$. For the hBeta model we set $a_0 = 1$.

For each segmentation \vec{d} , our method produces posterior predictive samples for 4 variables, $(u_{m+1,10}, u_{m+1,9}, u_{m+1,j_1}, u_{m+1,j_2})$. As our model explicitly assumes a Uniform density within each segmentation, the values of the remaining 6 continuous variables, $u_{m+1,j}$ for $j = 1 \cdots 8$ with $j \neq j_1$ and $j \neq j_2$, is sampled with equal probabilities from $\{\frac{1}{32}, \frac{3}{32}, \dots, \frac{31}{32}\}$. The posterior predictive sample, $(u_{m+1,1}^1 \cdots u_{m+1,10}^1), \dots, (u_{m+1,1}^n \cdots u_{m+1,10}^n)$, is then generated by importance sampling on $\vec{d} \in \mathcal{D}$. Lastly, we produce the posterior predictive sample, $(x_{m+1}^1, \vec{y}^1), \dots, (x_{m+1}^n, \vec{y}^n)$ as follows. $x_{m+1}^i = b$ if $u_{m+1,9}^i = 3/4$, $x_{m+1}^i = c$ if $u_{m+1,10}^i = 3/4$, otherwise $x_{m+1}^i = a$. While, for $j = 1 \cdots 8$ and $i = 1 \cdots n$, $y_{m+1,j}^i$ is sampled from the Uniform distribution on subinterval I_k^j , with $k = (u_{m+1,j}^i \cdot 32 + 1)/2$.

Note that the normalizing transformation applied to the continuous variables, ensures that the marginal posterior predictive distribution of Y_j , $j = 1 \cdots 8$, will be similar to the marginal distribution of Y_j even if U_j is not included in \vec{d} . However, to ensure that the marginal posterior predictive distribution of X will be similar to the marginal distribution of X , variables U_{10} and U_9 had to be included in each segmentation.

In Figure 8 we display the logarithm of numerator of Expression (2), which is proportional to the segmentation probability $\Pr(\vec{d}|\vec{u})$, for the 1960 segmentations in \mathcal{D} . The plot reveals that only the segmentations with continuous variables Y_1 and Y_2 had non-negligible selection probabilities. Thereby implying that the posterior predictive samples of $Y_3 \cdots Y_8$ were generated independently from a marginal distribution that is very similar to that of the original sample.

For all $\vec{d} \in \mathcal{D}$ we set $d_1 = 10$ and $d_2 = 9$, because according to our intuition beginning the segmentation with U_{10} and U_9 is supposed to yield the largest segmentation probability. To test our intuition, $\forall \vec{d} \in \mathcal{D}$, we compare the segmentation probability of $\vec{d} = (d_1 \cdots d_{10})$ to the segmentation probability of $\vec{d}' = (d'_1 \cdots d'_{10})$ derived by setting $d'_j = d_{j+2}$ for $j = 1 \cdots 8$, $d'_9 = 10$, $d'_{10} = 9$. And indeed, for all \vec{d} this change decreased the logarithm of the segmentation probabilities by more than 100.

The sample of observations, $x_1 \cdots x_{400}$, consisted of 216 observations with $X = a$, 111 observations with $X = b$, 73 observations with $X = c$. The posterior predictive sample of the categorical variable, $x_{401}^1 \cdots x_{401}^{1000}$, consisted of 535 observations with $X = a$, 327 observations with $X = b$, 138 observations with $X = c$. In Figure 9 we compare the joint conditional distribution of Y_1 and Y_2 , given $X = a$ and $X \neq a$, for the original sample and for the posterior predictive sample. Figure 9 reveals that our method

managed to pick up the relation between X , Y_1 and Y_2 , in $\tilde{\pi}$. While according to the results shown in Figure 8, our method also correctly modelled the independence in $\tilde{\pi}$ between Y_j , $j = 3 \cdots 8$, and the other variables.

6 Discussion

We presented a Bayesian framework for density estimation and predictive inference that is based on multiple random dyadic segmentations of the P -dimensional unit cube. To apply our methodology to a sample of m realizations of random vector $\vec{X} \in \mathbb{R}^P$, it is necessary to specify a mapping for each coordinate of \vec{X} into $[0, 1]$, set the value of a_0 and the segmentation level L , and specify the set of segmentations \mathcal{D} .

Our working experience suggests setting $a_0 = 1$. Our focus in this work is recovering the dependence between the components of $\vec{X} = (X_1 \cdots X_P)$. For small P , a linear mapping between an interval, slightly larger than the support of X_j , and $[0, 1]$ should be satisfactory. For larger P , the mapping we applied in Section 5, based on the empirical distribution of the variable, allowed us to recover the marginal distribution of a continuous variable X_j without including it in the segmentation.

For the simulated examples, we considered segmentations in which all subintervals at the same level were partitioned according to the same coordinate (therefore $|\mathcal{D}|$ was of order L^P) and we evaluated the posterior predictive distribution by importance sampling over all $\vec{d} \in \mathcal{D}$. This is not computationally feasible for large P . To overcome this problem we plan to consider a richer family of segmentations \mathcal{D} , in which the subintervals in the same level may be partitioned in different directions, and to evaluate the posterior predictive distribution by MCMC algorithms that perform random walks on \mathcal{D} .

The most interesting property of our method, illustrated in the simulated examples, is that it favours segmentations for which the step-function density approximates the distribution of \vec{X} well, and yields a step-function density that is easy to estimate by a Polya tree. We plan to provide theoretical support for this observation, which we will try to formalize as conjectures. Note that each segmentation \vec{d} of $[0, 1]^P$ into the level L subintervals, $\mathcal{I}_{L,1}(\vec{d}) \cdots \mathcal{I}_{L,2^L}(\vec{d})$, specifies a mapping from $[0, 1]^P$ to $\{1, 2, \dots, 2^L\}$ (see Figure 1 and top row of plots in Figure 5). We conjecture that \vec{d} for which distribution $\tilde{\pi}$ is increasing with respect to this mapping have larger posterior probabilities; provide smaller approximation error; yield increasing step-function densities that are easier to estimate.

References

- [1] Ferguson, T. S. (1974) "Prior distributions on spaces of probability measures," *Annals of Statistics*, 2, 615-629.
- [2] Ma, L. (2017) "Adaptive Shrinkage in Polya Tree Type Models", *Bayesian Analysis* 12, 3,779-805.
- [3] Vovk, V., Gammerman, A., Shafer, G. (2005) "Algorithmic Learning in a Random World." Springer.
- [4] Wong, W. H., Ma, L. (2010) "Optional Polya tree and Bayesian inference" *Annals of Statistics*, 38(3): 1433-1459.

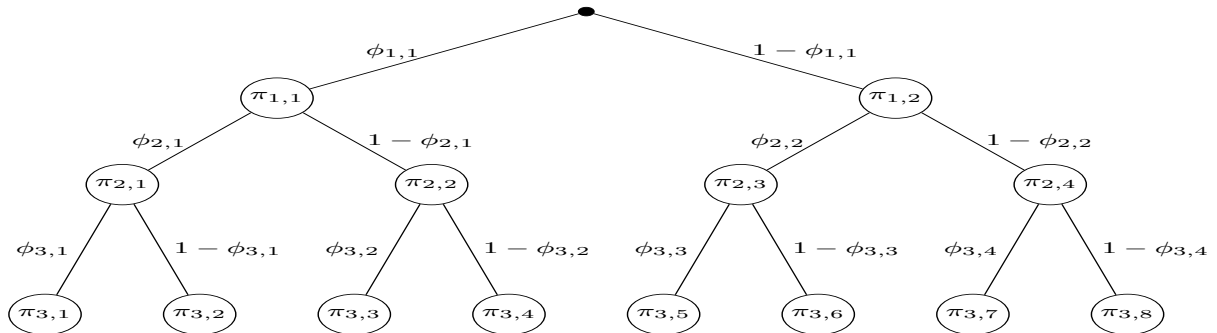


Figure 2: 3 level hierarchical Beta model. $\phi_{1,1}, \phi_{2,1}, \dots, \phi_{3,4}$ are independent Beta random variables. For $l = 1 \dots 3$ and $j = 1 \dots 2^l$, the probability $\pi_{l,j}$ is the product of the Beta random variables on the edges connecting it to the root node (solid black circle). The probabilities at level 3 specify the step function PDF for a dyadic partition of $[0, 1]^P$.

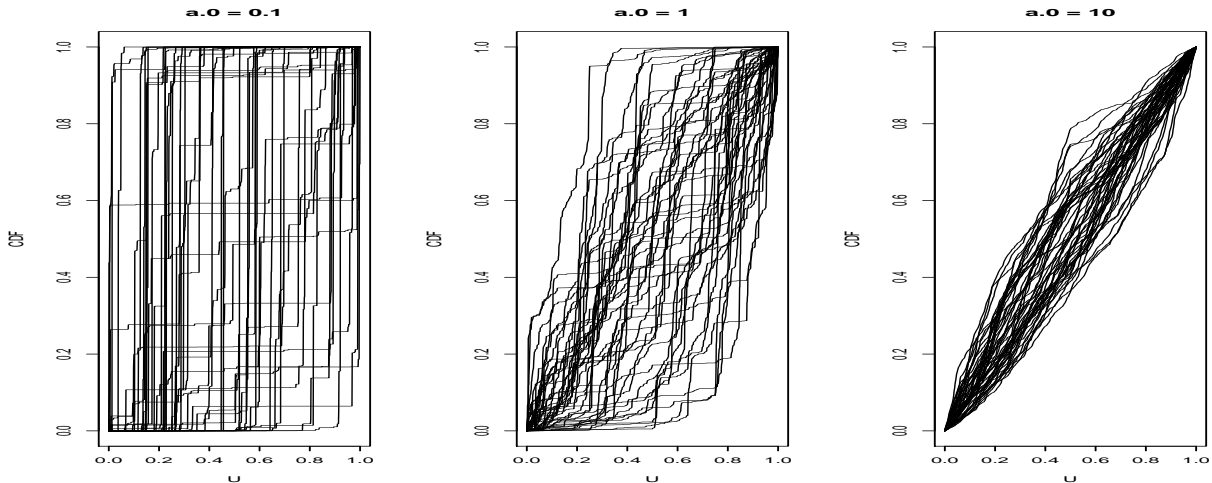


Figure 3: Generative model distribution of the step-function density. The plots display the CDF of step function $f(u|\vec{d}, \vec{\pi}_L)$ in Model 2.1, for the 10 level segmentation of $[0, 1]$ with $a_0 = 0.1$ (left plot), $a_0 = 1$ (middle plot), $a_0 = 10$ (right plot). Each plot consists of curves that display the CDF of $f(u|\vec{d}, \vec{\pi}_{10})$ for 50 realizations of $\vec{\pi}_{10}$. The X coordinates for each curve are the endpoints of the subintervals of $[0, 1]$: $0, \frac{1}{1024}, \dots, \frac{1023}{1024}, 1$. The Y coordinates for each curve are the cumulative sums of $\vec{\pi}_{10}$: $0, \pi_{10,1}, \pi_{10,1} + \pi_{10,2}, \dots, 1$.

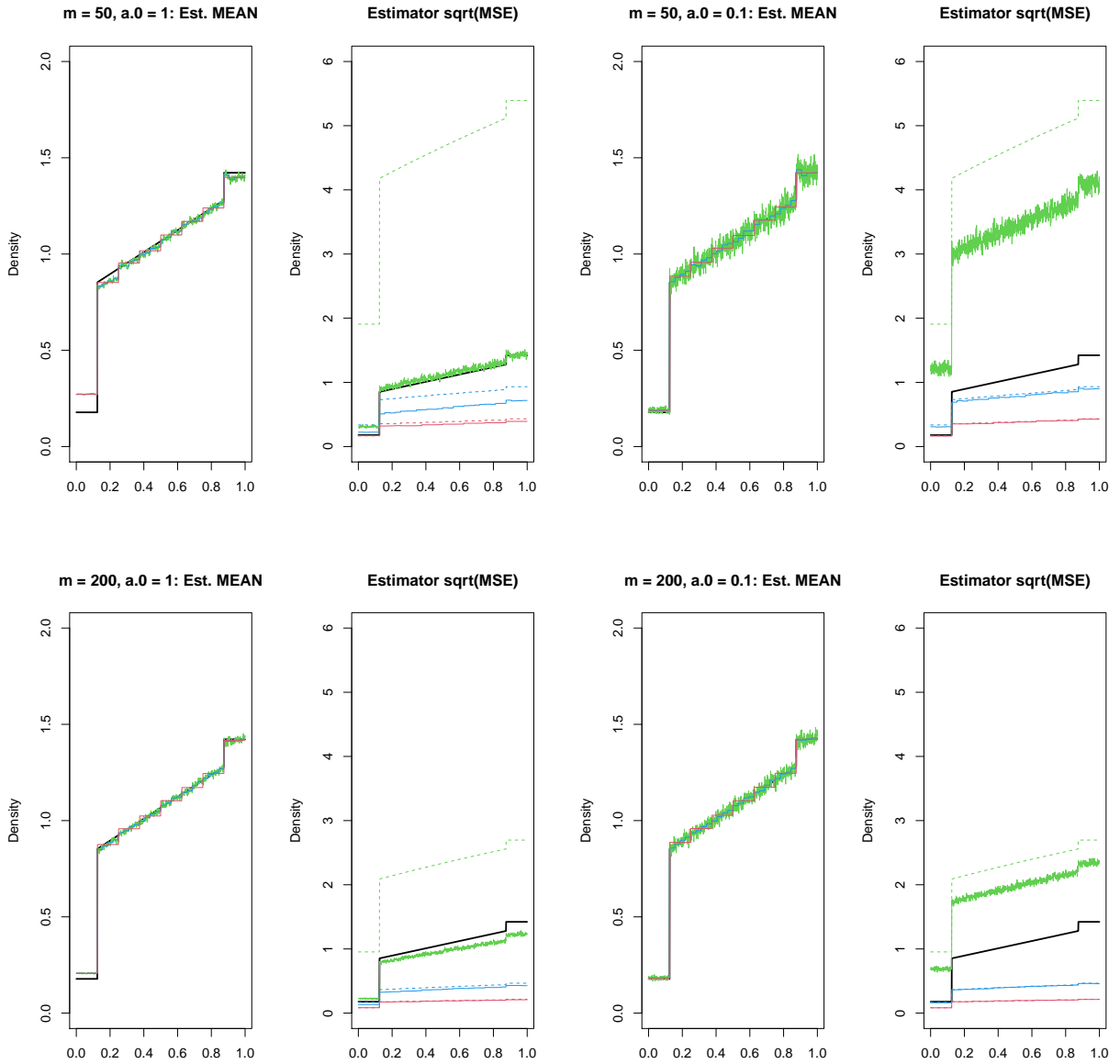


Figure 4: 1D density estimation – results of 4 simulations with $m = 50, 200$ and $a_0 = 1, 0.1$. Each pair of plots corresponds to the same simulations: the left plot is the simulation mean of the estimators; the right plot is the square root of the simulation MSE of the estimators. The black curve in all the plots is $\tilde{\pi}(u)$. The green, blue, red curves correspond to $L = 10, 5, 3$ level segmentation of $[0, 1]$. The solid curves correspond to hBeta estimators; the dashed curves are the square-root MSE for the interval-counts density estimators.

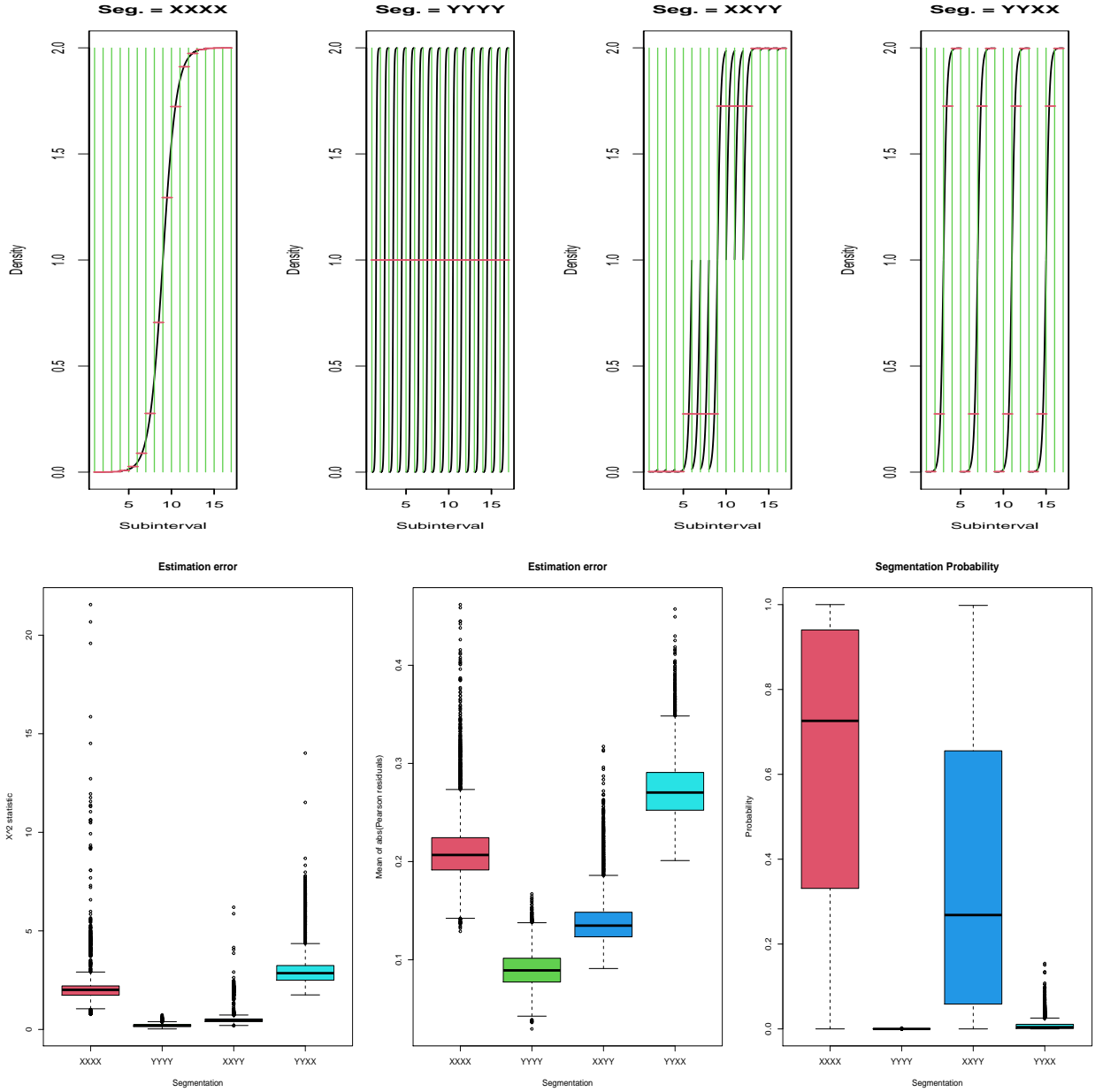


Figure 5: 2D density estimation – approximation error and simulation results for the four segmentations of $[0, 1]^2$ shown in Figure 1. The plots on the top row show how well $\tilde{\pi}(u_x, u_y)$ is approximated by $f(u; \vec{d}, \tilde{\pi}_L)$ for each segmentation. In each plot, the regions between the green lines correspond to the 16 subintervals of each segmentation; the black curves display the profile of $\tilde{\pi}(u_x, u_y)$ and the red lines display $f(u; \vec{d}, \tilde{\pi}_L)$ in each subinterval of each segmentation. The boxplots in the bottom row display simulation results. The left and middle sets of boxplots display the distribution of X^2 and the distribution of the mean of the absolute value of the Pearson residuals, for the four segmentations. The four boxplots on the right display the distribution of $\Pr(\vec{d}|\vec{u})$ for each segmentation.

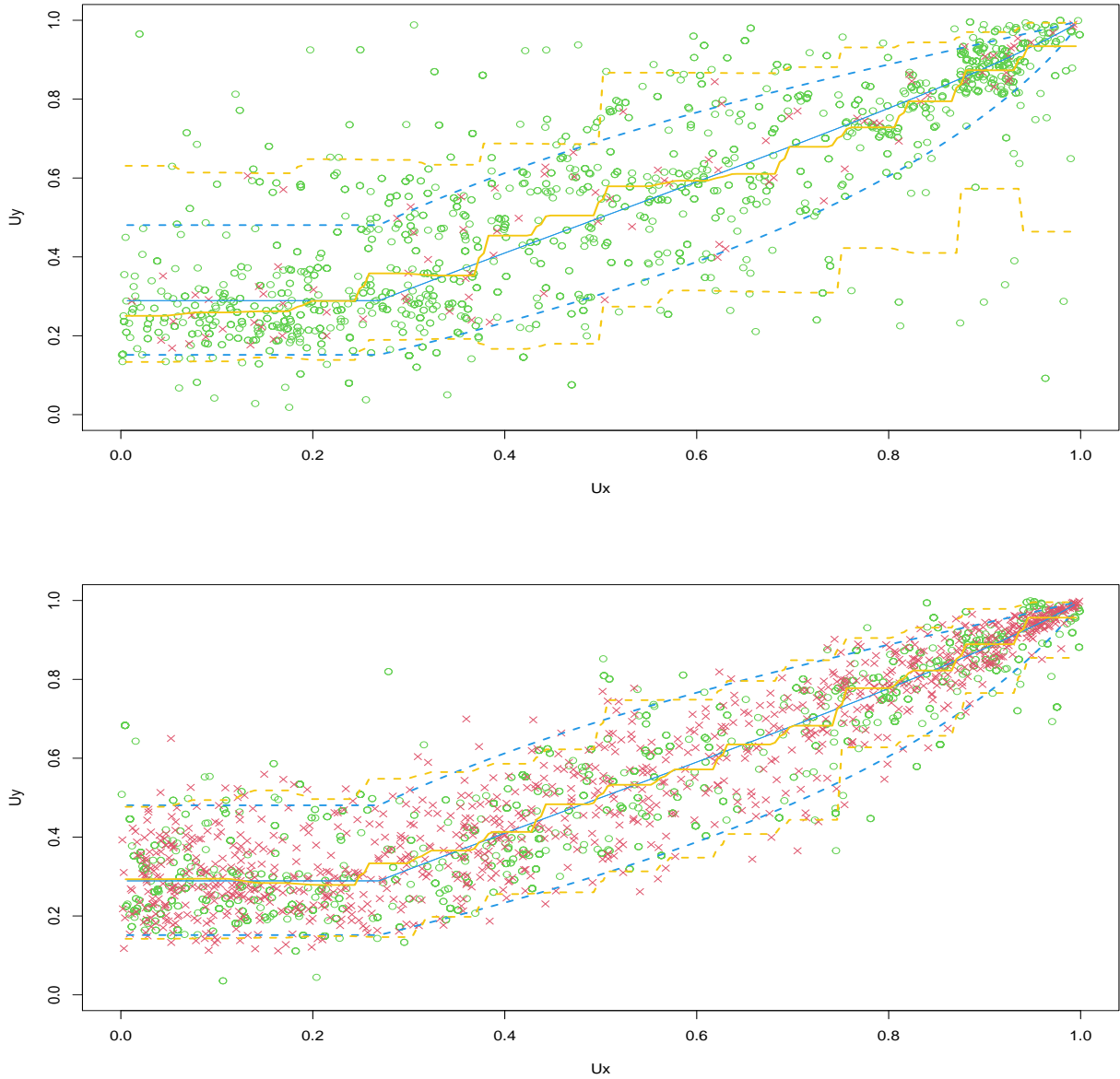


Figure 6: Quantile regression simulated example – Credible Prediction Sets. The plots correspond to simulations with sample size $m = 100$ (top) and $m = 1000$ (bottom). The Red X's mark the observations, $u_1 \cdots u_m$. The Green circles are posterior predictive samples, $u_{m+1}^1 \cdots u_{m+1}^{2000}$. The solid Blue curves mark the conditional median of U_y given U_x , the dashed blue curves mark the 0.05 and 0.95 quantiles of the conditional distribution of U_y given U_x . The Orange curves are the the 0.05 and 0.95 quantiles and median of the conditional posterior predictive distribution of U_y given U_x .

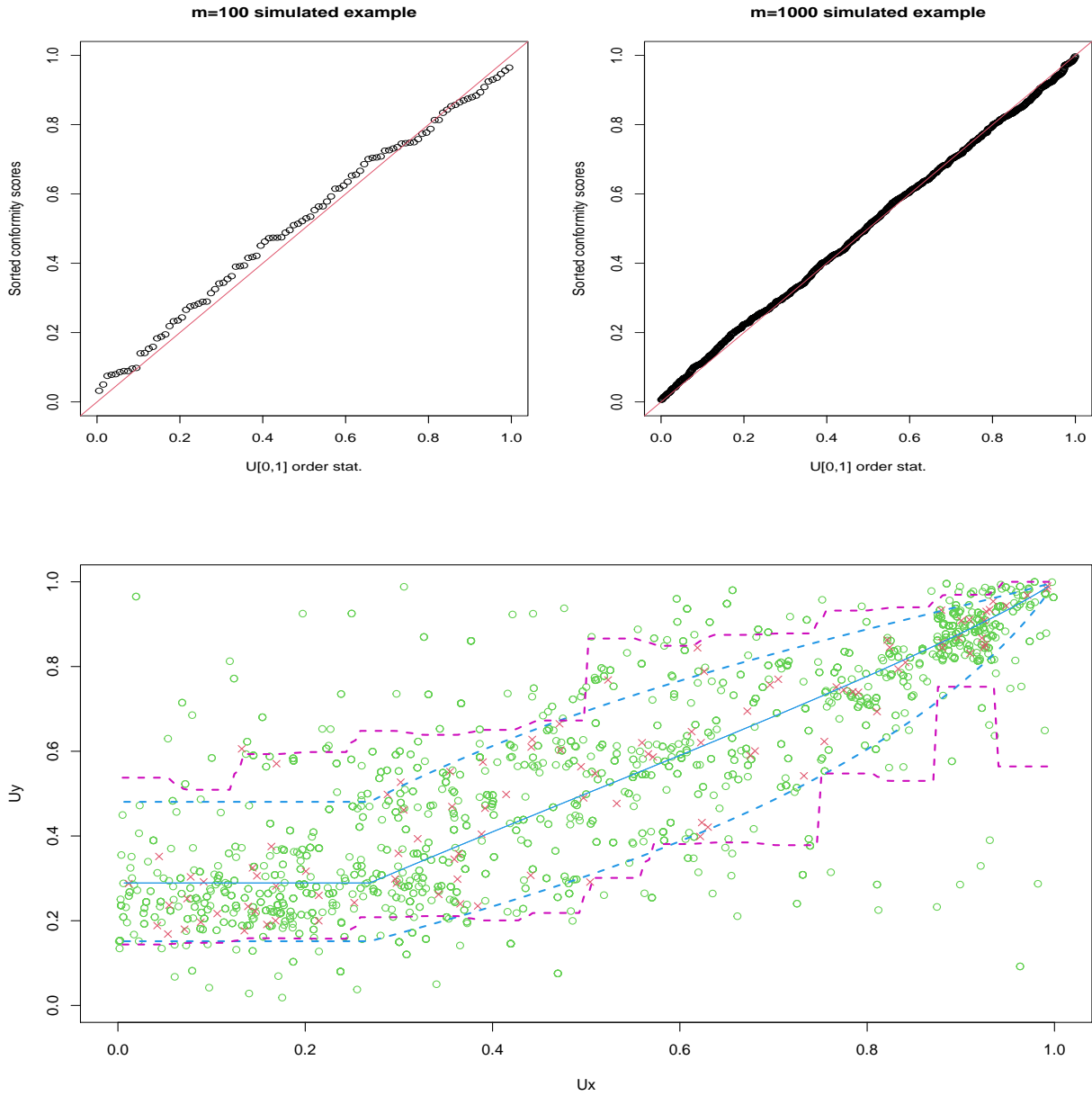


Figure 7: Quantile regression simulated example – Conformal Prediction Sets. The plots in the top row are $U[0, 1]$ qqplots for the conformity scores of the m observations for the simulated examples shown in Figure 6. The Purple dashed curves in the bottom plot are 0.95 Conformal Prediction Set for u_{m+1} for the simulated example shown in the top plot of Figure 6 (the Red and Green points and blue curves are the same as in Figure 6).

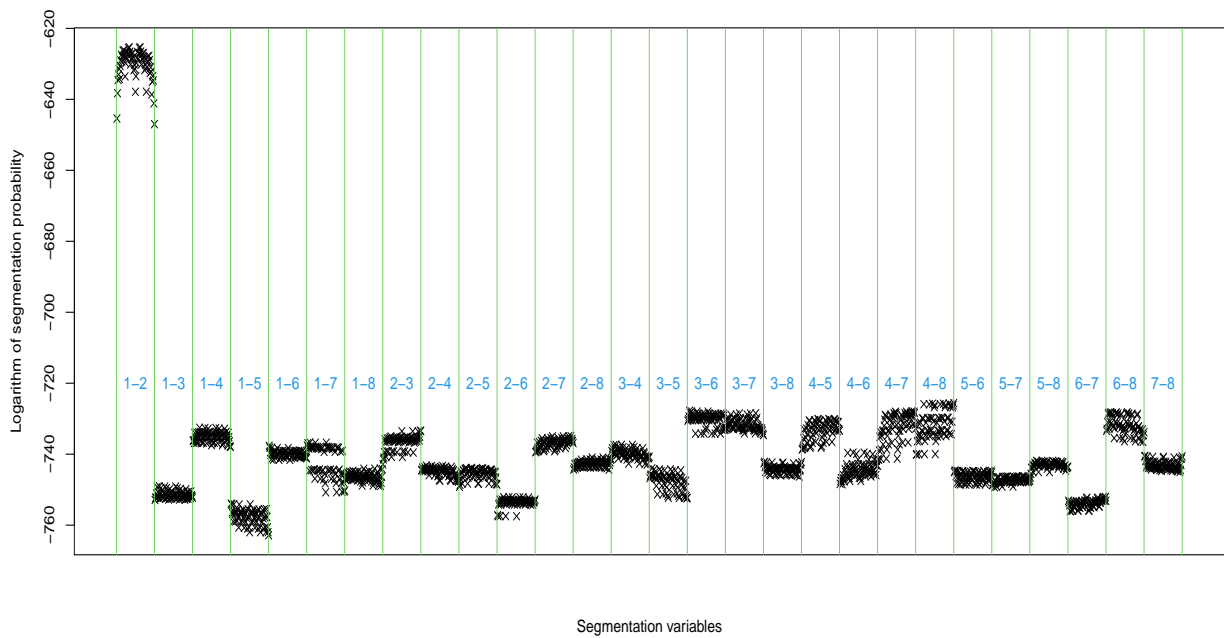


Figure 8: High Dimensional Predictive Inference simulation – Log-probability of the 1960 segmentations. The probabilities are arranged in 28 groups of 70 segmentations that correspond to the pair of continuous variables listed in Blue.

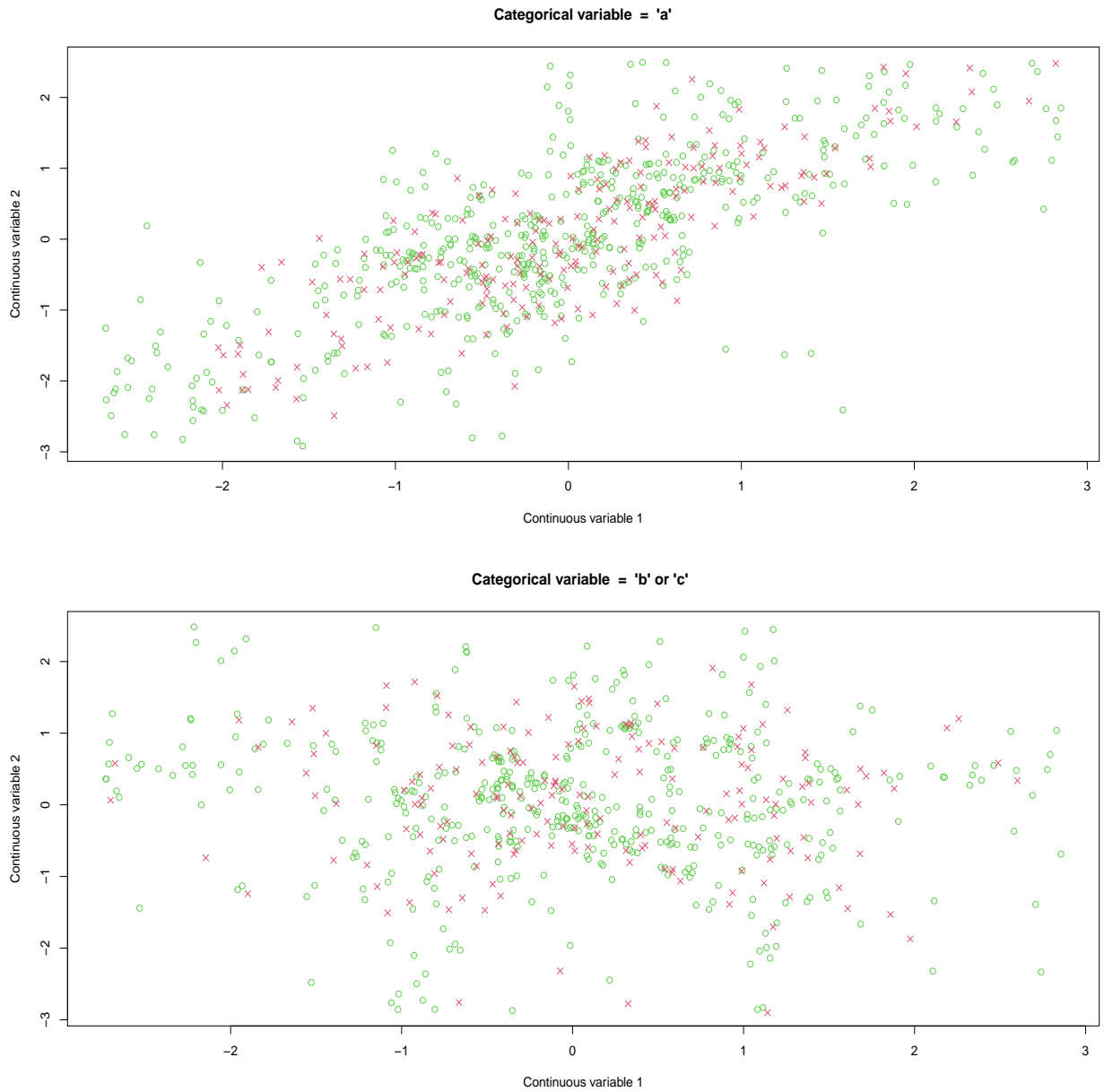


Figure 9: High Dimensional Predictive Inference simulation – joint distribution of X , Y_1 and Y_2 . The Red x signs form scatterplots for the first and second components of $\vec{y}_1 \cdots \vec{y}_{400}$, for $x_i = a$ (top plot), and for $x_i \neq a$ (bottom plot), $i = 1 \cdots 400$. The Green circles form scatterplots for the first and second components of the posterior predictive samples, $\vec{y}_{401}^1 \cdots \vec{y}_{401}^{1000}$, for $x_{401}^i = a$, and for $x_{401}^i \neq a$, $i = 1 \cdots 1000$.